Multifrequency EPR, ^{1}H ENDOR, and saturation recovery of paramagnetic defects in diamond films grown by chemical vapor deposition

D. F. Talbot-Ponsonby, M. E. Newton,* and J. M. Baker
Clarendon Laboratory, Department of Physics, University of Oxford, Parks Road, Oxford OX1 3PU, United Kingdom

G. A. Scarsbrook, R. S. Sussmann, and A. J. Whitehead
De Beers Industrial Diamond Division (UK) Ltd., Charters, Sunninghill, Ascot, United Kingdom

Susanne Pfenninger[†]
MACC Fund Research Center Building, Biophysics Section, Medical College of Wisconsin, 8701 Watertown Plank Road, Milwaukee, Wisconsin 53226

Paramagnetic defects in free-standing polycrystalline chemical vapor deposition (CVD) diamond films have been studied using multifrequency electron paramagnetic resonance (EPR) (1–35 GHz), electron-nuclear double resonance (ENDOR), saturation recovery, and infrared absorption. The results confirm the ^{1}H hyperfine parameters for the recently identified H1 defect [Zhou *et al.*, Phys. Rev. B **54**, 7881 (1996)]. However, in the CVD diamond samples studied here, H1 is always accompanied by another defect at $g = 2.0028(1)$. Saturation recovery measurements are consistent with two defects centered on $g = 2.0028$. At temperatures below 100 K the spin-lattice relaxation rate of H1 is determined by the direct process and is a factor of 10–100 times more rapid than the single substitutional nitrogen center, which is known to be incorporated into the bulk diamond. [1]H matrix ENDOR measurements indicate that the H1 center is in an environment with hydrogen atoms 0.2–1.0 nm from the center. The near-neighbor hydrogen identified by multifrequency EPR was not detected in the ENDOR experiments. The concentration of H1 correlates with the total integrated CH stretch infrared absorption in the samples studied here. All the evidence is consistent with H1 being located at hydrogen decorated grain boundaries (or in intergranular material) rather than in the bulk diamond. A third EPR resonance at $g = 2.0028(1)$ has been observed in some of the CVD diamond samples studied. The resonance is distinguished by its temperature-dependent linewidth: above 50 K the line is exchange narrowed, but below 50 K it broadens rapidly with decreasing temperature. [S0163-1829(98)03404-3]

I. INTRODUCTION

Hydrogen incorporation into diamond has been studied for many years. In natural type Ia diamond a sharp infrared absorption line at 3107 cm^{-1} has been attributed to a C-H stretch.[1] Recently, the creation of the 3107-cm^{-1} center has been reported in synthetic diamond grown at high temperature and pressures (HTP) by high-temperature annealing.[2] This result indicates that hydrogen may be incorporated into HTP synthetic diamond, in a form not so far detected, and migration of the hydrogen on annealing produces the defect with the local mode at 3107 cm^{-1}.

In recent years the incorporation of hydrogen into polycrystalline diamond films grown by chemical vapour deposition (CVD) has attracted considerable attention. The 3107-cm^{-1} absorption has not been reported in CVD diamond films. However, infrared absorption studies have revealed several different CH stretch vibrations in the region 2750–3300 cm^{-1} arising from carbon-hydrogen bonds in different environments.[3,4] The CH stretch signatures of hydrogen bonded to sp^2-bonded carbon appear above 2950 cm^{-1}, while those associated with sp^3-bonded carbon appear below 3000 cm^{-1}. Other absorptions are often present at frequencies [2820 and 2833 cm^{-1} (Refs. 3 and 4)] below those normally observed for CH stretching vibrations in amorphous hydrogenated carbon. These have tentatively been associated with nitrogen and oxygen defects,[4] or hydrogen bonded directly on a diamond (111) surface.[3] McNamara *et al.*[4] have suggested that at low concentrations (less than 0.2 at. %) the hydrogen content is consistent with the hydrogen being located at grain boundaries and when the bulk concentration is higher in amorphous hydrogenated carbon in between grains. High-quality CVD diamond films show little or no CH related absorption in the region 2750–3300 cm^{-1}.

A grain boundary, which separates identical crystallites, is a two-dimensional extended defect that contains point defects. In polycrystalline silicon the silicon dangling bond defect at a grain boundary has been identified, and passivation of this defect with hydrogen has been studied.[5] The formation and dissociation of a grain boundary point defect, possibly consisting of an isolated hydrogen atom at the bond-center site of a prestrained Si-Si bond, has been postulated as being responsible for changes in the electrical conductivity of polycrystalline silicon.[6] The unique properties of diamond (optical transparency, thermal conductivity, radiation hardness, etc.) have encouraged interest in the fabrication of polycrystalline diamond electronic devices (e.g., uv-blind photoconductive detectors[7] and particle detectors[8]). If these applications are to succeed, a thorough understanding of

electrically active point defects at grain boundaries is required.

An electron paramagnetic resonance (EPR) defect centered on $g = 2.0028(1)$ is commonly observed in polycrystalline CVD diamond.[9–14] Observations at the X band (8–12 GHz) sometimes reveal partially resolved satellites separated by 1.25 ± 0.15 mT at 9.6 GHz and centered on $g = 2.0028$. Measurements on the position and intensity of the satellites made at approximately 35 GHz, taken together with the X-band data, suggested that they arise from forbidden nuclear-spin-flip transitions of a hydrogen atom weakly coupled to the unpaired electron spin.[13]

Studies of the satellite separation at microwave frequencies between 1 and 9.6 GHz showed that the satellites did not originate from forbidden spin-flip transitions with a hydrogen atom with a vanishingly small hyperfine coupling to the unpaired electron.[14] As well as the commonly observed $g = 2.0028$ center, the sample used for the multifrequency EPR study (1–9.6 GHz) discussed above[14] contained another EPR center not previously reported with $g = 2.0028(1)$, a temperature-dependent linewidth, and a non-Curie-law temperature dependence of the EPR intensity. This was not initially understood. In the light of the data reported here and recently by other workers,[15,16] we now believe that the biradical model,[14] which appeared to explain satisfactorily the microwave frequency dependence of the satellite separation and the spectral line shape in this range of microwave frequency (1–9.6 GHz), is incorrect.

Zhou *et al.*[15,16] analyzed the EPR absorption at $g = 2.0028$ in several different CVD diamond films at microwave frequencies between 9.8 and 35 GHz and concluded from simulations of the EPR line shape that the EPR absorption was due to a single well-defined defect consisting of an unpaired electron coupled to a hydrogen atom ~ 0.2 nm away. They proposed that this defect (labeled H1) was created by a hydrogen atom entering a stretched C-C bond at a grain boundary, allowing the carbons to relax back, one bonding to the hydrogen and the other with an unpaired electron predominately localized in its dangling bond. The hydrogen hyperfine coupling parameters used in the powder simulation of the line shape were $A_\parallel = 27.5(2.5)$ MHz and $A_\perp = -5.5(2.5)$ MHz. At microwave frequencies above 9.6 GHz the intensity of the satellites is primarily controlled by the square of the magnitude of the anisotropic component of the hyperfine coupling $[b = (A_\parallel - A_\perp)/3 = 11.0$ MHz$]$. Simulation of the narrow central line of the spectrum requires $A_\perp$ to be small, which necessitates a nonzero isotropic hyperfine coupling $[a = (A_\parallel + 2A_\perp)/3 = 5.5$ MHz$]$.

We present EPR data on a range of CVD diamond samples. The low-frequency EPR measurements show that in the samples we have studied the line shape of the EPR absorption at $g = 2.0028$ cannot be explained by H1 alone and at least one other defect with a resonance at $g = 2.0028$ is also present. It is very difficult to establish the presence of this other center from EPR data at microwave frequencies of 9 GHz and above.

II. EXPERIMENT

A. Growth and characterization

The free-standing polycrystalline diamond films were grown by microwave-plasma chemical vapor deposition under a variety of different synthesis conditions to obtain a range of samples. The diamond films were characterized by Raman and infrared absorption. The Raman measurements were obtained at room temperature with a Renishaw Ramascope incorporating a charge coupled device detection system and excitation at 633 nm. The infrared absorption measurements were made with a Perkin-Elmer 1710 Fourier transform infrared spectrometer, at room temperature.

B. EPR and ENDOR spectrometer

Continuous-wave EPR measurements were made at 1.2, 1.8, 2.3, 3.5, 5.8, 9.6, and 34–35.0 GHz. The spectrometers operating at frequencies between 1.2 and 5.8 GHz were all constructed and operated at the National Biomedical ESR Center.[17] They all utilized a loop-gap resonator as the microwave element.[18] Measurements were made at temperatures down to 100 K by inserting the loop-gap resonator into a Varian Q-band nitrogen flow dewar. The spectrometer operating at 9.6 GHz was constructed in the Clarendon Laboratory and incorporated a standard reference arm microwave bridge. The magnetic field was generated using a Varian 9-in. electromagnet, with an EPS10/1 electromagnet power supply and MS-10/GPIB magnetic field controller designed and constructed at the Technical University of Wroclaw. A Bruker TE$_{104}$ cavity was used with an Oxford Instruments ESR900 cryostat at temperatures between 4 and 300 K. Double integration of the first-harmonic EPR signal and comparison with a reference sample allowed bulk spin concentrations to be determined. The reference used was a synthetic Ib diamond containing EPR active single substitutional nitrogen,[19] the concentration of which was determined by infrared absorption using the parameters determined by Woods *et al.*[20]

Two Q-band spectrometers were used. The EPR electron nuclear double resonance (ENDOR) spectrometer (34.5–35.5 GHz) was constructed in the Clarendon Laboratory and has been described in detail elsewhere.[21] ^{1}H ENDOR was detected at temperatures between 4 and 100 K via double phase-sensitive detection, initially at the field modulation frequency (115 kHz) and then at the radio-frequency (rf) frequency modulation frequency (87 Hz). The cylindrical ENDOR cavity operated in the TE$_{011}$ mode with a single-turn rf coil that ran the length of the cavity and was about 3 mm wide. The rf coil was terminated with a 50-Ω load and the maximum rf power used was 20 W. The second Q-band EPR spectrometer (33.8–34.2 GHz) was a standard Bruker instrument, with a variable temperature (77–350 K) probe-head assembly (ER5102 QT). Data acquisition was controlled by a personal computer interfaced to the Bruker ER200D console.

Measurements of spin-lattice relaxation times (T_1) were made at approximately 9.3 GHz using the saturation recovery spectrometer at the National Biomedical ESR Center.[17] Low microwave observe power was used to minimize the distortion of T_1 and the impact of spectral diffusion on the saturation recovery data was tested with measurements as a function of the length of the pump pulse.
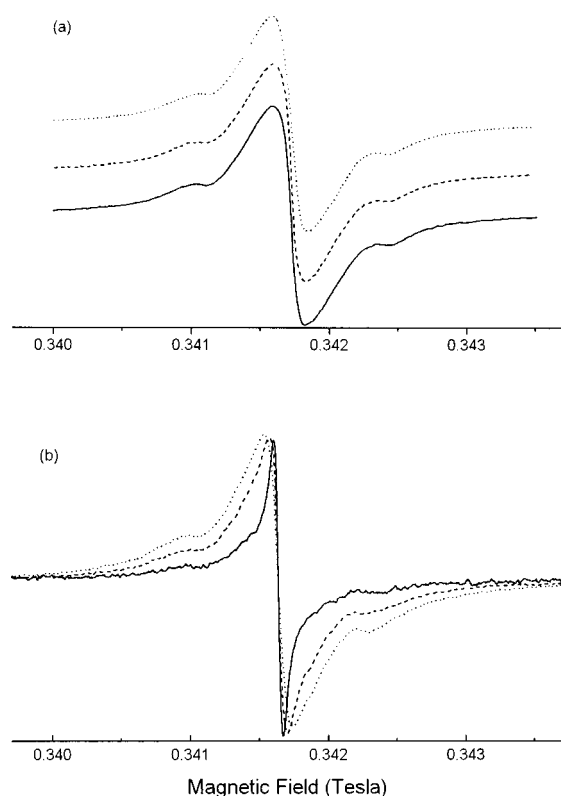
FIG. 1. *X*-band (9.6-GHz) EPR spectra from CVD diamond sample (a) type *A* at 298 K (solid line), 117 K (dashed line), and 5.2 K (dotted line) and (b) type *B* at 150 K (solid line), 60 K (dashed line), and 5 K (dotted line). Spectra are recorded under conditions of low microwave power to avoid saturation and low modulation amplitude to avoid distortion of the line shape.

III. RESULTS

A. Raman and infrared absorption measurements

All films exhibited the first-order diamond Raman peak at 1332 cm^{-1}. The full width at half height varied from 2.3 to 6.0 cm^{-1} in different samples. A weak broad structure was observed in the range 1200–1600 cm^{-1} in most samples, which has been attributed to double- or triple-bonded carbon.[22] The infrared absorption in the CH region showed for all samples studied that the CH stretch signatures of hydrogen bonded to sp^3-bonded carbon dominated the absorption (ignoring fundamental diamond absorption). The total integrated CH stretch absorption in the region 2750–3300 cm^{-1} for each sample is given in Fig. 2.

B. EPR and infrared measurements

Figure 1(a) shows the *X*-band EPR spectra centered on $g = 2.0028(1)$ typical of most of the polycrystalline CVD diamond samples we have studied (for ease of reference we will refer to these samples as type *A*) and are similar to many spectra reported in the literature. We and other workers find that the resolution of the satellites is sample dependent. As shown in Fig. 1(a), the line shape is temperature independent and in addition the EPR intensity follows the Curie law. The degree of resolution of the satellites does not correlate with either the total concentration of paramagnetic defects or the total integrated CH absorption strength. Figure 1(a) is similar
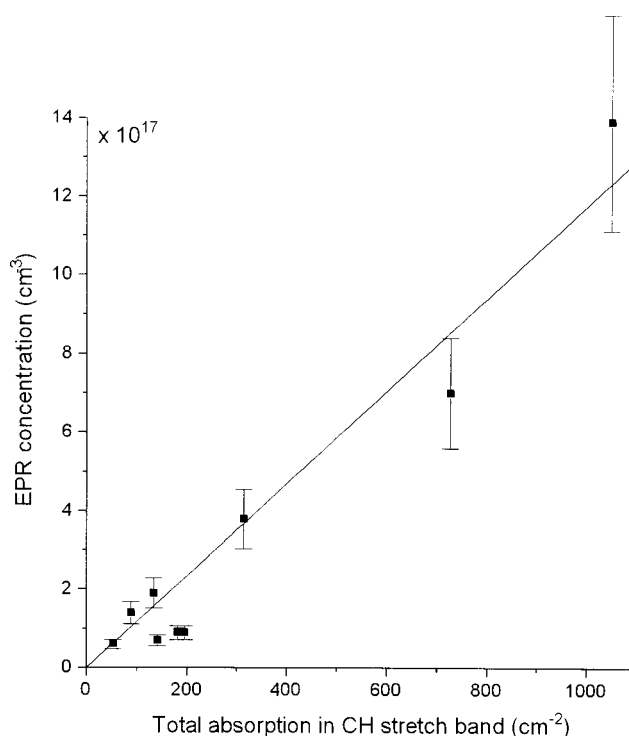

FIG. 2. Integrated EPR spin concentration (excluding any contribution from the single substitutional nitrogen center) plotted against integrated absorption in the CH region of infrared spectrum.

to the *X*-band EPR spectrum shown by Zhou *et al.*,[15,16] but the satellites are weaker relative to the central line.

Figure 1(b) shows *X*-band EPR spectra from the specimen studied in detail by Talbot-Ponsonby *et al.*;[14] for ease of reference we will refer to these samples as type *B*. Unlike type-*A* samples, the line shape of the EPR absorption from type-*B* samples shows a marked temperature dependence. The EPR absorption is dominated by a narrow line centered on $g = 2.0028(1)$ at high temperature, but as the temperature is decreased this line broadens rapidly. At low temperatures the EPR spectrum is dominated by the spectrum observed in type-*A* samples.

Figure 2 shows the EPR spin concentration measured at 5 K, less any contribution from the single substitutional nitrogen defect,[19] which is an impurity in some CVD diamond samples, plotted against the total integrated absorption in the CH stretch region of the infrared spectrum for the nine samples studied. The EPR concentration from the species centered on $g = 2.0028$ correlates with the total infrared absorption in the CH stretch region, but there is no correlation with the single substitutional nitrogen concentration.

Unambiguous interpretation of EPR spectra taken at a single microwave frequency is often difficult. Figure 3 shows the results of measurements at 1.2, 3.4, 9.6, and 34.0 GHz on a type-*A* sample. The calculated H1 EPR spectra at these microwave frequencies are shown alongside the experimental data in Fig. 3. The 34.0-GHz data appear to be in good agreement with the H1 model. However, as the microwave frequency is reduced, the model fails to reproduce the experimental data.

C. ^{1}H ENDOR

Observation of hydrogen spin-flip satellites centered on $g = 2.0028$ stimulated a ^{1}H ENDOR study of the hydrogen
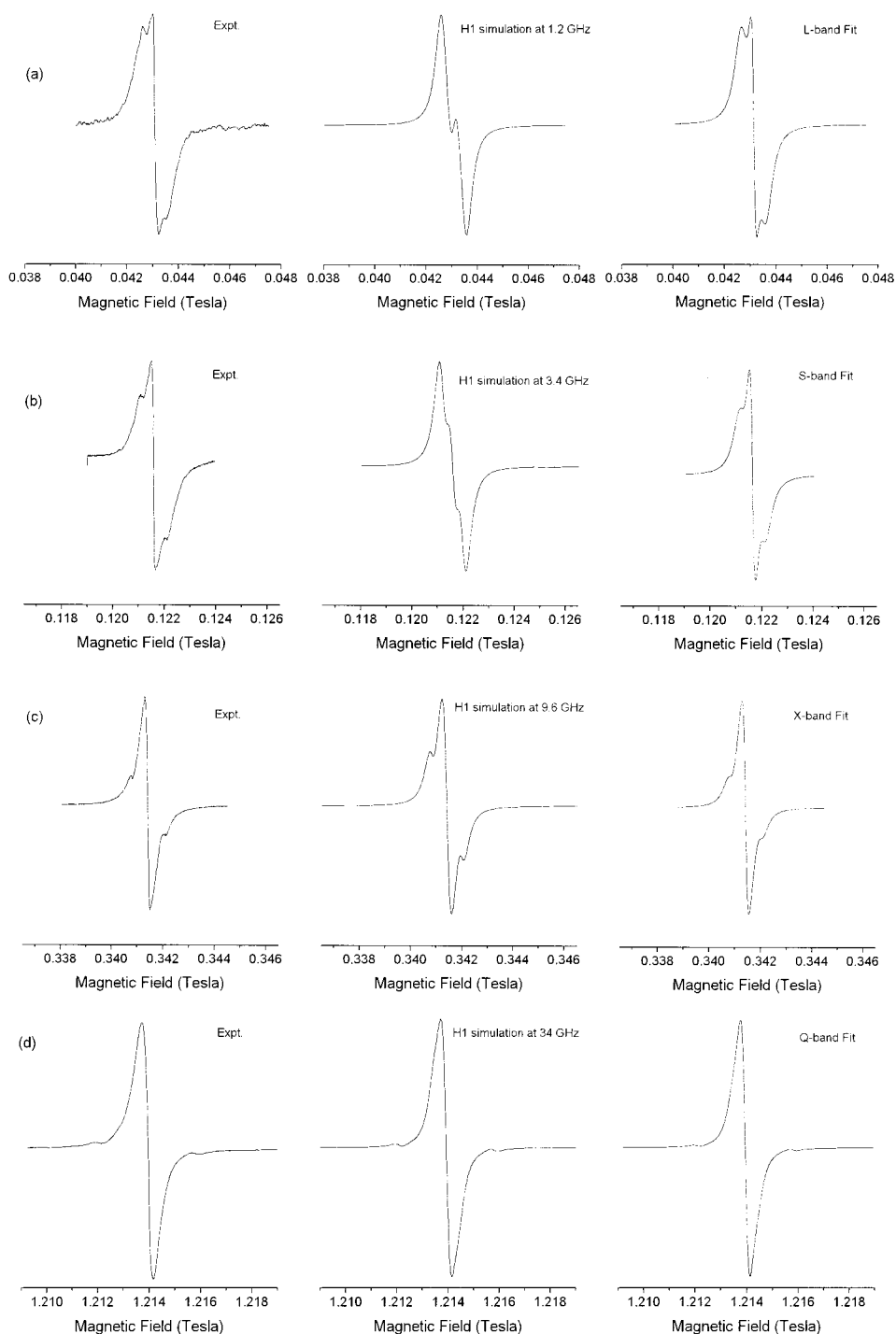
FIG. 3. EPR spectra obtained from a type-A sample (see the text for details) at microwave frequencies of (a) 1.2 GHz, (b) 3.4 GHz, (c) 9.6 GHz, and (d) 34 GHz. The sample temperature was 100 K and spectra were recorded under conditions of low microwave power to avoid saturation and low modulation amplitude to avoid distortion of the lineshape. Alongside each experimental spectrum is the simulation of the H1 EPR spectrum at the specified microwave frequency. Powder simulation used a Lorentzian line shape with full width at half height of 0.30 mT. On the far right of each row is the fit derived from the $H1$ defect [half-width at half height (HWHH) 0.30 mT] plus an additional Lorentzian resonance at $g = 2.0028(1)$ (HWHH 0.22 mT). The EPR linewidth and the relative intensity of the two components is fixed for all frequencies.

atom(s) neighboring the unpaired electron. The ENDOR detection scheme detailed in Sec. II B produces first derivative line shapes: Fig. 4 shows the integrated ENDOR spectrum obtained from a type-A sample at 5 K. The ENDOR resonance is centered on the ^{1}H nuclear Zeeman frequency [calculation of the nuclear g factor 5.59(1) from the nuclear

resonant frequency and the magnetic field confirms that this is a proton resonance] and is typical of ^{1}H matrix ENDOR signals observed in disordered solids.[23] The hyperfine parameters for the unique hydrogen neighbor of the H1 center determined by analysis of the EPR line shape[16] were used to calculate the position of ENDOR resonances expected from
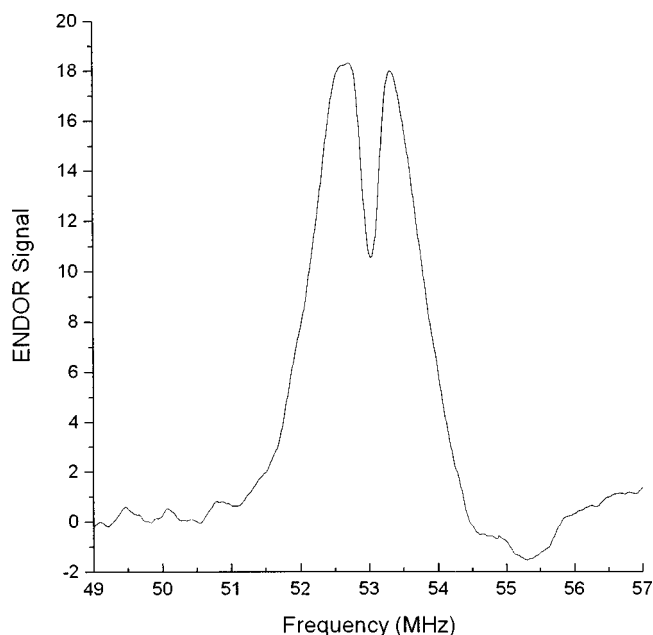
FIG. 4. ENDOR spectrum obtained from a type-*A* sample. The temperature is 4.5 K, microwave frequency 34.85 GHz, microwave power 2 mW, and rf power 20 W. The spectrum is recorded using double lock-in detection at field modulation frequency (115 kHz) and rf frequency modulation frequency (87 Hz) and integrated to produce absorption signal.

this hydrogen atom. Despite a thorough investigation at and around the frequencies predicted by calculation, no ENDOR signals attributable to the unique hydrogen neighbor of H1 were observed. The ^{1}H matrix ENDOR signal was detected at temperatures up to 100 K without any appreciable change in line shape. However, the signal-to-noise ratio diminished appreciably with increasing temperature. At 5 K a ^{1}H matrix ENDOR signal could be detected with the magnetic field set to resonance at $g = 2.0028$ in all type-*A* and type-*B* samples studied.

D. Saturation recovery measurements

Detection of continuous-wave ENDOR signals is dependent on achieving an appropriate balance of relaxation rates. The temperature dependence of the spin-lattice relaxation rate was studied between 10 and 100 K using the technique of saturation recovery. All of the methods of measuring the electron spin-lattice relaxation rates are complicated by the necessity of eliminating the effects of spectral diffusion. Spectral diffusion leads to a spreading of saturation over the inhomogeneously broadened line. Spectral diffusion contributes to the recovery from saturation by the observed spin packet in competition with intrinsic spin-lattice relaxation processes. The importance of spectral diffusion can be assessed by observation of the recovery from saturation as a function of saturating pulse length. Experiments on type-*A* samples showed that the recovery was not well described by a single exponential; a better fit could be obtained with a combination of two exponentials. The dependence of the two relaxation rates determined by fitting the data to two exponentials on the saturating pulse length is shown in Fig. 5(a). For short pulses spectral diffusion significantly affects the measured recovery rates. As the saturating pulse length is
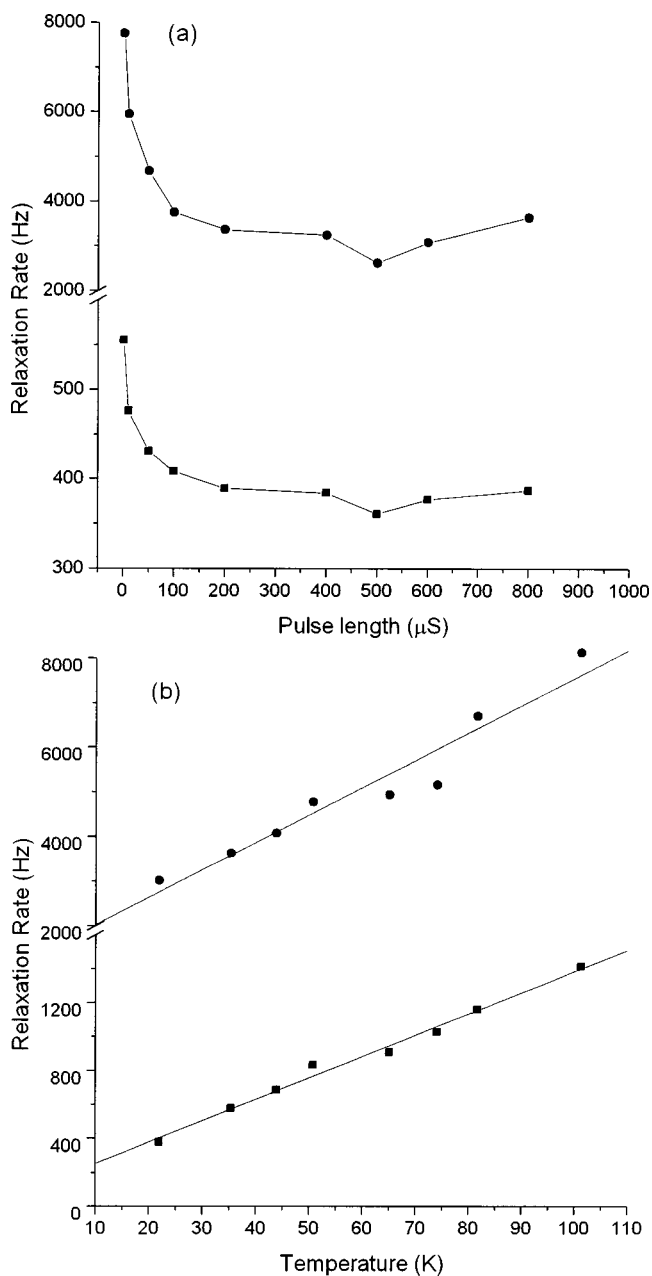

FIG. 5. (a) Dependence of the relaxation rates for the $g = 2.0028$ EPR resonance in a type-*A* CVD diamond sample at 20 K, obtained by fitting the saturation recovery response to a sum of two exponential functions, on the duration of the saturating microwave pulse. (b) Temperature dependence of the relaxation rates determined as described in (a) with a saturating pulse length of 400 μS. Solid lines are a linear fit to the observed dependence.

increased the spectral-diffusion channels are progressively saturated. Figure 5(b) shows the variation of the relaxation rates of the two components of the recovery with temperature (400-μs saturating pulse).

IV. DISCUSSION

The H1 center

The multifrequency EPR (9.8–35 GHz) data presented in Fig. 1 of Zhou *et al.*[15,16] was satisfactorily reproduced by the H1 defect (with a sample-dependent linewidth) without any

other components. The low-frequency EPR data presented in Fig. 3 are not reproduced by the H1 center alone. However, a convincing fit can be obtained at all frequencies using the H1 defect plus an additional isotropic resonance at $g = 2.0028$. The experimental data and fits are shown in Fig. 3. The asymmetry in the experimental data shown in the Q-band data [Fig. 3(d)] probably indicates a small anisotropy in the g matrix. The additional isotropic resonance at $g = 2.0028$ has a Lorentzian line shape, a full width at half height of 0.22(2) mT, and is present at the same relative intensity at all microwave frequencies. The measurements at low and high microwave frequencies showed no evidence of g-strain broadening, which would originate from a spread in g values caused by random local strains.

EPR investigations indicate that the H1 defect is a commonly observed defect. Studies of the EPR line shape as a function of microwave frequency permit the identification of the neighboring hydrogen atom and its hyperfine coupling parameters. Our data confirm the parameters $b = 11.0(2.5)$ MHz and $a = 5.5(2.5)$ MHz, determined by Zhou *et al.*[15,16] We can find no other model that is consistent with all the experimental data. The X-band and Q-band data presented in Fig. 3 could be fitted using a model similar to H1, with smaller hyperfine parameters and no additional component; however, these parameters do not reproduce the low-frequency data, which unambiguously indicate the presence of an additional resonance at $g = 2.0028$. It appears that the relative concentrations of H1 and the additional EPR center are sample dependent. We cannot rule out the possibility that this additional resonance is the H2 center identified by Zhou *et al.*[15,16] We have not observed H2 in the absence of H1 in any sample we have studied. Observation of satellites belonging to H2 is impossible when H1 is strong. The lack of information makes speculation on the origin of the additional resonance unwarranted.

For all samples from which data are shown in Fig. 2, the H1 defect makes the dominant contribution to the total unpaired electron concentration. The correlation between the concentration of H1 and the total CH infrared absorption is consistent with H1 being located on hydrogen decorated grain boundaries or in hydrogenated nondiamond material in between the grain boundaries. We have shown that in the samples labeled type A the absorption at $g = 2.0028$ originates from two defects. In surveying over 20 samples we have not found one that contains only H1.

The assumption that the H1 center is located in hydrogenated regions of the sample is supported by observation of a ^{1}H ENDOR line at the free nuclear frequency. This line originates from hydrogen atoms surrounding the unpaired electron and weakly coupled to it via the electron-nuclear dipolar interaction. It is usually referred to as the ^{1}H matrix ENDOR line.[23] The dip in the center of the line arises from nuclear coherence effects and suggests the presence of more than one ^{1}H neighbor.[24] Information about the distribution of the unpaired electron and the local environment can be extracted from the matrix ENDOR line shape.[23] A simple but useful model for the line shape assumes a uniform ^{1}H distribution and contains only two parameters: the lower limit of the electron-proton separation (separation above which only a dipolar interaction need be considered) and the width of the nuclear spin packet.[25] Following this approach, we

find that the experimental matrix ENDOR line shape is best reproduced with this simple model with a lower limit of separation of the order of the next-nearest-neighbor separation in diamond (0.25 nm), if we assume that the nuclear spin-packet half width at half height is 200 kHz, which is in accord with previous observations.[26] We note that NMR studies show that the majority of the hydrogen in diamond films gives rise to a Gaussian NMR signal with a full width at half maximum of 50–70 kHz.[27] However, it is well known that NMR line shapes are not characteristic of the nuclear line shapes appropriate to matrix ENDOR. Matrix ENDOR detects only those nuclei near a paramagnetic species. For these nuclei the nuclear relaxation time will be less than for the bulk nuclei and hence the nuclear line will be broader.

No ^{1}H ENDOR lines were observed from the unique hydrogen neighbor (at 0.19 nm) of the H1 center identified by analysis of the EPR line shape. This negative result suggests that the matrix ENDOR response is much stronger than that of the near neighbor. This is not unreasonable since the matrix ENDOR response probably arises from many ^{1}H neighbors that all add to the resonance around the nuclear Zeeman frequency, whereas the ENDOR intensity from the single near neighbor is spread out over several megahertz by the anisotropic component of its hyperfine interaction. No temperature dependence of the width of the ^{1}H matrix ENDOR signal could be detected up to 100 K; this is consistent with the hydrogen being rigidly bound.

In Sec. III D it was shown that spectral diffusion can significantly alter the measured saturation recovery rates. Two processes that contribute to spectral diffusion are electron spin-spin interactions that will occur on a time scale of the phase memory decay (T_2) and electron-nuclear spin-spin interactions that occur on a much slower time scale. For long saturating pulses, when the spectral diffusion channels are saturated, we found that the recovery was best fitted by a sum of two exponentials. For a given spin we would expect a single exponential recovery; hence one possible explanation of the two component decay is that the resonance at $g = 2.0028$ consists of two components with different spin-lattice relaxation rates. This is consistent with the multifrequency EPR data, which indicated the presence of H1 and another defect. At high microwave powers changes in the continuous-wave EPR line shape suggest that one defect is being preferentially saturated. This is consistent with the two defects having different relaxation rates, as shown in Fig. 5(b). The linear dependence of both relaxation rates with temperature indicates that the direct mechanism[28] dominates spin-lattice relaxation in this temperature region. In CVD diamond samples containing single substitutional nitrogen, continuous wave power saturation studies show that the spin-lattice relaxation rate for the nitrogen center is of order 10–100 times less than that for the H1 center.

The designation of a sample as type B requires the presence of a previously unreported EPR signal at $g = 2.0028(1)$ that has a temperature-dependent EPR linewidth. This is the third different EPR center with a g value of 2.0028(1) we have observed in CVD diamond. The dependence of the EPR linewidth on temperature indicates that the resonance is exchange narrowed at temperatures above about 50 K. As the temperature is reduced below 50 K the lifetime of magnetically distinguishable states increases and the EPR

linewidth broadens appreciably. The temperature dependence of the EPR signal was difficult to follow at low temperature because of overlapping resonances from the H1 defect and the other unidentified defect at $g = 2.0028$. The center is easily detected in the rapid exchange limit because the resonance is very narrow. Several different exchange mechanisms (e.g., electron exchange, electron transfer, and proton exchange) could be invoked to explain the observed phenomena. The paucity of information prohibits further speculation.

V. CONCLUSION

The EPR measurements reported here support the proposal of Zhou *et al.*[15,16] that the H1 center is a well-defined defect with a unique hydrogen neighbor about 0.19 nm away from the unpaired electron. However, the low-frequency EPR measurements show conclusively in all the samples we have studied that H1 is always accompanied by another defect at $g = 2.0028(1)$. No model has yet been proposed for this second defect, and we cannot rule out the possibility that it is the H2 center previously reported.[15,16] [1]H matrix ENDOR indicates that in addition to the near-neighbor hydrogen H1 is in an environment with other hydrogen atoms 0.2–1.0 nm away. The spin-lattice relaxation rate of H1 is much more rapid than that of the substitutional nitrogen center that is known to be incorporated into the diamond lattice. All the evidence is consistent with the H1 defect being located at grain boundaries, not in the bulk diamond. A third EPR resonance at $g = 2.0028(1)$ has been observed. This resonance is distinguished from the others by a temperature-dependent EPR linewidth. Studies on this center are in progress.

*Author to whom correspondence should be addressed.

†Present address: Kantonales Laboratorium für Lebensmittelkontrolle und Umweltschutz, Postfach 322, CH 8201 Schallhausen, Switzerland.

[1] G. S. Woods and A. T. Collins, J. Phys. Chem. Solids **44**, 471 (1983).

[2] I. Kiflawi, D. Fisher, H. Kanda, and G. Sittas, in *Diamond Conference, Cambridge, 1996*, edited by J. E. Field (De Beers Industrial Diamond Division, Ascot, 1996), p. 28.

[3] B. Dischler, C. Wild, W. Müller-Sebert, and P. Koidl, Physica B **185**, 217 (1993).

[4] K. McNamara, B. Williams, K. Gleason, and B. E. Scruggs, J. Appl. Phys. **76**, 2466 (1994).

[5] N. Johnson, D. Biegelsen, and M. Moyer, Appl. Phys. Lett. **40**, 882 (1982).

[6] N. Nickel, N. Johnson, and C. Van de Walle, Phys. Rev. Lett. **72**, 3393 (1994).

[7] L. Allers and A. T. Collins, J. Appl. Phys. **77**, 3879 (1995).

[8] A. Mainwood *et al.*, J. Phys. D **28**, 1279 (1995).

[9] I. Watanabe and K. Sugata, Jpn. J. Appl. Phys., Part 1 **27**, 1808 (1988).

[10] W. Zhang, F. Zhang, Q. Wu, and G. Chen, Mater. Lett. **15**, 292 (1992).

[11] M. Fanciulli and T. D. Moustakas, Phys. Rev. B **48**, 14 982 (1993).

[12] H. Jia, J. Shinar, D. P. Lang, and M. Pruski, Phys. Rev. B **48**, 17 595 (1993).

[13] S. L. Holder, L. G. Rowan, and J. J. Krebs, Appl. Phys. Lett. **64**, 1091 (1994).

[14] D. Talbot-Ponsonby *et al.*, J. Phys.: Condens. Matter **8**, 837 (1996).

[15] X. Zhou, G. Watkins, and K. M. McNamara-Rutledge, Mater. Sci. Forum **196-201**, 825 (1996).

[16] X. Zhou, G. Watkins, K. M. McNamara-Rutledge, R. P. Messmer, and Sanjay Chawla, Phys. Rev. B **54**, 7881 (1996).

[17] National Biomedical ESR Center, Medical College of Wisconsin, MACC Fund Research Center Building, 8701 Watertown Plank Road, Milwaukee, WI 53226. WWW: http://www.biophysics.mcw.edu/BRI-EPR.

[18] W. Froncisz and J. S. Hyde, J. Magn. Reson. **47**, 515 (1982).

[19] W. V. Smith, P. P. Sorokin, I. L. Gelles, and G. J. Lasher, Phys. Rev. **115**, 1546 (1959).

[20] G. S. Woods, J. Wyk, and A. T. Collins, Philos. Mag. B **62**, 589 (1990).

[21] D. Twitchen *et al.*, Phys. Rev. B **54**, 6988 (1996).

[22] M. Mermoux *et al.*, Diamond Relat. Mater. **1**, 519 (1992).

[23] L. Kevan and L. Kispert, *Electron Spin Double Resonance Spectroscopy* (Wiley-Interscience, New York, 1976).

[24] J. Freed, D. S. Leniart, and J. Hyde, J. Chem. Phys. **47**, 2762 (1967).

[25] J. Hyde, G. Rist, and L. Eriksson, J. Phys. Chem. **72**, 4269 (1968).

[26] J. Baker and M. Newton, Appl. Magn. Reson. **7**, 209 (1994).

[27] K. M. McNamara, D. H. Levy, K. K. Gleason, and C. J. Robinson, Appl. Phys. Lett. **60**, 580 (1992).

[28] A. Abragam and B. Bleaney, *Electron Paramagnetic Resonance of Transition Ions* (Dover, New York, 1986).